# Insertion of singlet chlorocarbenes across C–H bonds in alkanes: Evidence for two phase mechanism*

M RAMALINGAM,[1,**] K RAMASAMI[2] and P VENUVANALINGAM[3]

[1]Department of Chemistry, Rajah Serfoji Government College, Thanjavur 613 005
[2]Department of Chemistry, Nehru Memorial College, Puthanampatti 621 007
[3]School of Chemistry, Bharathidasan University, Tiruchirapalli 620 024
e-mail: m_ramlingam@yahoo.com

**Abstract.** Transition states for the insertion reactions of singlet mono and dichlorocarbenes ($^1$CHCl and $^1$CCl$_2$) into C–H bonds of alkanes (methane, ethane, propane and *n*-butane) have been investigated at MP2 and DFT levels with 6-31g (*d*, *p*) basis set. The $p_\pi$ of $^1$CHCl and $^1$CCl$_2$ may interact with alkane's filled fragment orbital of either $\sigma$ or $\pi$ symmetry. So chlorocarbenes insertion reactions have been investigated for both ($\sigma/\pi$) approaches. The $\sigma$ approach has been adjudicated to be the minimum energy path over the $\pi$ approach both at the MP2 and DFT levels. Mulliken, NPA and ESP derived charge analyses have been carried out along the minimal energy reaction path using the IRC method for $^1$CHCl and $^1$CCl$_2$ insertions into the primary and secondary C–H bonds of propane. The occurrence of TSs either in the electrophilic or nucleophilic phase has been identified through NBO charge analyses in addition to the net charge flow from alkane to the carbene moiety.

**Keywords.** Singlet chlorocarbenes insertion; C–H of alkanes; MP2 and DFT; NBO analysis.

## 1. Introduction

The hydrochloroflurocarbons (HCFCs) and hydro-flurocarbons (HFCs) with a shorter lifetime of a few months are slowly phasing out the refrigerants chloro-fluorocarbons (CFCs) and halogens which are potent stratospheric ozone destroyers.[1] The advantages of HCFCs and HFCs are their susceptibility to quick oxidation by OH radicals in the troposphere and their photodissociation to halocarbenes. In addition to their importance in atmospheric chemistry, halocarbenes (:CXY) and carbenes are important transient intermediates in organic synthesis,[2] in organometallic chemistry[3] and in gas phase combustion.[4,5] Regarding the stability the large $\sigma - p_\pi$ separation[6–8] and inductive/mesomeric effects make the halocarbenes more stable in the singlet state. The vacant $p_\pi$ orbital and the fully occupied $\sigma$ orbital on the carbenic carbene are responsible for their electrophilic and nucleophilic reactions respectively.[9] Among the different types of reactions of singlet carbenes, the highly characteristic concerted insertion reactions into Y–H bonds (Y=C, Si, O, etc.), involving a three-center cyclic transition

state[10] seem to be important in synthetic organic chemistry.[2] The electrophilicity of carbenes has been reported to decrease with increased chlorination[8] resulting in a substantially high activation barrier as reported in the case of fluorocarbenes.[11] The present investigation focuses on the mechanism of $^1$CHCl and $^1$CCl$_2$ insertion into the primary and secondary C–H bonds of methane, ethane, propane, and *n*-butane (scheme 1) and characterize the electrophilic and nucleophilic nature of the chlorocarbenes in these insertion reactions. If the total charge on the chlorocarbene moiety as the reaction progresses (by IRC[12]) is monitored one could detect the 'turning point' that will mark the end of the first phase (electrophilic phase) and the onset of the second (nucleophlic phase). In order to gain evidence for the two-phase
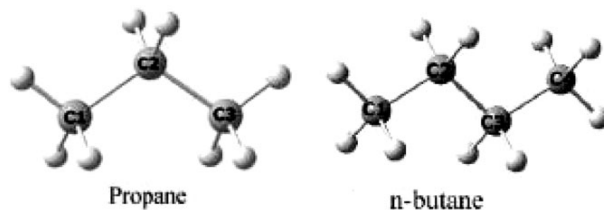


**Scheme 1.** Compounds and numbering system adopted in this study.

**Table 1.** Activation barriers (in kcal/mol) for insertion of $^1CHCl$ and $^1CCl_2$ into alkanes at B3LYP/6-31g(*d, p*) and MP2/6-31g(*d, p*) levels for sigma (pi) orientations.

| | CHCl | | $CCl_2$ | |
|---|---|---|---|---|
| | B3LYP | MP2 | B3LYP | MP2 |
| Methane | 4·87 (5·15) | 7·05 (7·35) | 20·57 (21·44) | 18·83 (19·83) |
| Ethane | 1·27 (1·82) | 3·47 (3·67) | 15·66 (16·97) | 12·98 (14·30) |
| Propane (C1) | 1·37 (1·80) | 3·22 (3·35) | 15·90 (17·38) | 12·60 (14·17) |
| Propane (C2) | 0·69 (0·50) | 0·79 (1·39) | 12·45 (13·80) | 8·59 (10·24) |
| *n*-Butane (C1) | 1·21 (2·29) | 3·05 (3·44) | 15·48 (17·21) | 11·94 (13·91) |
| *n*-Butane (C2) | 0·69 (0·73) | 0·76 (1·05) | 12·62 (14·80) | 7·95 (10·30) |
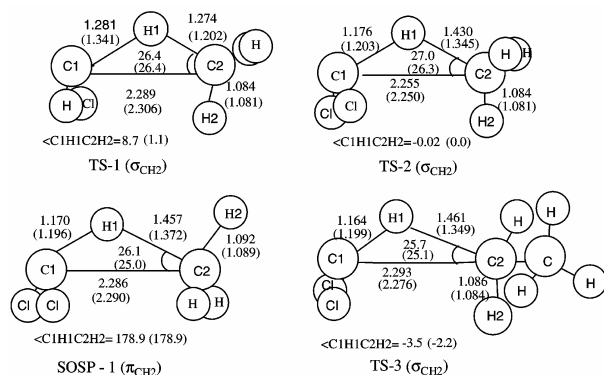


**Figure 1.** Selected optimized geometrical parameters (distances in Å and angles in degrees) of the transition states at B3LYP/6-31g (*d, p*) and MP2/6-31g (*d, p*) (in parentheses) levels.

mechanism, the charge versus reaction path probe for the insertion reactions into the primary and secondary C–H bonds of propane have been carried out. As the transient carbenes are short lived, *ab initio* quantum mechanical investigations of the carbene reactions are helpful in bringing out the insights and complement the experimental techniques in understanding the reaction mechanism.

## 2. Method of calculations

This investigation was performed with Gaussian03W suite of program.[13] The geometries of the chlorocarbenes, the alkane substrates, the transition states and the products have been optimized initially at HF/6-31g (*d, p*) level. The resultant geometries were then taken as inputs for MP2 and B3LYP[14–18] investigations. For a better treatment of 1,2-hydrogen shift during the insertion process, standard 6-31g (*d, p*)[19,20] basis set has been adopted. In all the $\pi$-approaches the

carbenic–carbon and the atoms of the –CHR-unit of the alkane bearing the hydrogen that undergoes shift to the nucleophilic face of the carbene were constrained to be in one plane during the geometry optimization. The harmonic vibrational frequency calculations at MP2 and B3LYP levels were carried out to characterize all the stationary points as either minima, first-order saddle points or second-order saddle points – SOSP. Following the location of the relevant transition state, the IRC was followed using the Schlegel–Gonzalez algorithm.[21] The Mulliken,[22] NPA[23] and charges derived by fitting the electrostatic potential (CHelpG)[24] methods have been followed for the atomic charges computations, along the reaction path.

## 3. Results and discussion

### 3.1 *Singlet chlorocarbenes insertions into methane and ethane*

The activation barriers computed at B3LYP/6-31g (*d, p*) and MP2/6-31g (*d, p*) levels are listed in table 1. The $p_\pi$ of $^1CHCl$ and $^1CCl_2$ may interact with alkane's filled fragment orbital of either $\sigma$ or $\pi$ symmetry. So chlorocarbenes insertion reactions have been investigated for both ($\sigma/\pi$) approaches and the $\sigma$ approach has been adjudicated to be the minimum energy path resulting in a staggered conformer. Our recent investigation of fluorocarbenes insertion[11] and the earlier report of carbene[25] and oxygen insertions[26] into C–H, also preferably assume $\sigma$ orientation over the $\pi$ approach. The σ approaches of $^1CHCl$ and $^1CCl_2$ towards the C–H of methane are associated with the activation barriers of 4·87 and 20·57 kcal/mol respectively at B3LYP/6-31g (*d, p*) (table 1). The MP2/6-31g (*d, p*) value for $^1CHCl$ insertion is ∼ 2 kcal/mol higher and that for $^1CCl_2$ insertion is ∼ 2 kcal/mol lower than those of the corresponding

B3LYP/6-31g (*d*, *p*) values. Replacement of hydrogen by chlorine in ${}^1$CHCl decreases its electrophilicity.[27] So the barrier heights increase from 4·87 to 20·57 kcal/mol at B3LYP and 7·05 to 18·83 kcal/mol at MP2 calculations respectively for methane. Both in the $\sigma$ and the $\pi$ orientations the enhanced nucleophilicity of ethane seems to be the reason for the barrier height lowering through ~3·3 to 3·7 kcal/mol for ${}^1$CHCl insertion. Similarly, the barrier height for ${}^1$CCl$_2$ into ethane does show the same trend (a reduction through ~4·5 to 5·9 kcal/mol). This aspect is clear from the fact that the reactivity decreases as the chlorination increases in the carbene. The predominant $\pi$-donation over $\sigma$-attraction by chlorine atom could be the reason for this enormous increase in the activation barrier with the degree of chlorination. Over all, the $\sigma_{CH_2}$ orientation for ${}^1$CHCl (${}^1$CCl$_2$) insertion has been found to be slightly preferred over the $\pi_{CH_2}$ approach. The relevant geometrical parameters of the transition states for the ${}^1$CHCl and ${}^1$CCl$_2$ insertions in $\sigma$ and $\pi$ orientations have been shown in figure 1. The TS for ${}^1$CCl$_2$ insertion (TS-2) comes much later along the reaction coordinate than that for ${}^1$CHCl insertion (TS-1) as reflected in the relative C2–H1 bond distances of 1·430 (1·345) and 1·274 (1·202) Å and the charges on H1 of 0·284(0·260) and 0·253 (0·225) a.u. respectively.

## 3.2 *Singlet chlorocarbenes insertions into C–H of higher alkanes*

The B3LYP and MP2 barrier heights for these have been listed in table 1. For the $\sigma$-insertion of ${}^1$CHCl into the primary C–H of ethane to *n*-butane, the barrier heights calculated at B3LYP/6-31g (*d*, *p*) have been found to be around 1·3 kcal/mol. But MP2 predictions (~3·2 kcal/mol) are slightly higher by ~1·9 kcal/mol. The small reduction in barrier height on moving from methane to ethane (3·5 kcal/mol) should have been due to the enhanced nucleophilicity by the methyl substituent in methane and this effect is insignificant on further increasing the hydrocarbon chain length. When we investigated the insertion pathway for secondary C–H, the barrier heights have been found to be appreciably reduced to an average value of ~0·69 kcal/mol at B3LYP level and ~1·22 kcal/mol at MP2 level. The proximity of the electron donating alkyl group to the insertion site is the reason for this result. If the carbene is ${}^1$CCl$_2$ the barrier height decreases to ~16·9 kcal/mol at DFT for all primary C–H insertions on comparison with that for

methane and it falls around 14·1 kcal/mol at MP2 level. The decreased electrophilicity may be the reason for the enhanced barrier heights. This trend also reveals that the steric factor has no noticeable influence upon the insertion pathway. For secondary C–H, the barrier heights have been found to be reduced to an average value of ~0·78 kcal/mol and 8·27 kcal/mol for insertion of ${}^1$CHCl and ${}^1$CCl$_2$ respectively at MP2 level. The proximity of the electron donating alkyl group to the insertion site might be the reason for this result.

## 3.3 *Energetics*

In the case of insertion of ${}^1$CHCl and ${}^1$CCl$_2$ into an alkane, the activation barrier is higher for primary than secondary C–H bonds (table 1). The above trend draws support from the fact that the pair of electrons on the carbene–carbon involved in the bonding process is more and more stabilized with the degree of chlorination. Due to the less availability of the electron pair on the carbene–carbon, ease of bond formation is inhibited. The NBO[28] (Natural bond orbital) analyses quantify this aspect in terms of the energies of the electron pairs on ${}^1$CHCl and ${}^1$CCl$_2$ as –0·4057 and –0·5595 a.u. at B3LYP and –0·4535 and –0·6019 a.u. at MP2 respectively. The enthalpies of chlorocarbene insertion reactions calculated from the equation (table 2),

$$\Delta_r H^0(298\ \mathrm{K}) = \sum(\varepsilon_0 + H_{\mathrm{corr}})_{\mathrm{products}}$$
$$-\sum(\varepsilon_0 + H_{\mathrm{corr}})_{\mathrm{reactants}},$$

$\varepsilon_0$ is the total electronic energy; $H_{\mathrm{corr}}$ the correction to the enthalpy due to internal energy.

All the reaction enthalpies show the exothermicity of the insertion reactions indicating that all the tran-

**Table 2.** Heat of reaction (kcal/mol) for insertion of singlet chlorocarbenes into C–H bonds of alkanes using 6-31g (*d*, *p*) at B3LYP and MP2 levels.

| Alkane | CHCl | | CCl$_2$ | |
|---|---|---|---|---|
| | B3LYP | MP2 | B3LYP | MP2 |
| Methane | –77·72 | –94·82 | –62·92 | –78·25 |
| Ethane | –79·31 | –97·63 | –64·48 | –81·38 |
| Propane (C1) | –79·14 | –97·66 | –64·29 | –81·48 |
| Propane (C2) | –79·83 | –99·75 | –63·89 | –82·79 |
| *n*–Butane (C1) | –79·14 | –97·73 | –64·31 | –81·59 |
| *n*–Butane (C2) | –78·73 | –99·09 | –62·47 | –82·88 |

**Table 3.** Selected geometrical parameters (distances in Å, angles in degrees, and barriers in (kcal/mol) at the TSs of $^1$CHCl with alkanes at B3LYP (MP2)/6-31g($d$, $p$).

| Alkane | $r_{C1H1}$ | $r_{C1C2}$ | $r_{C2H1}$ | $\theta_{H1C1C2}$ | $\theta_{H1C2C1}$ | $\phi_{C1H1C2H2}$ | $q_{ct}$ |
|---|---|---|---|---|---|---|---|
| Methane | 1·281 | 2·289 | 1·274 | 26·2 | 26·4 | 8·7 | 0·237 |
| | (1·341) | (2·306) | (1·202) | (23·5) | (26·4) | (1·1) | (0·193) |
| Ethane | 1·296 | 2·343 | 1·260 | 23·2 | 23·9 | 12·0 | 0·2527 |
| | (1·409) | (2·401) | (1·173) | (19·6) | (23·8) | (9·8) | (0·161) |
| Propane (c1) | 1·295 | 2·340 | 1·261 | 23·4 | 24·1 | 9·5 | 0·2531 |
| | (1·416) | (2·406) | (1·172) | (19·6) | (23·9) | (4·6) | (0·157) |
| Propane (c2) | 1·290 | 2·421 | 1·272 | 18·9 | 19·2 | 43·2 | 0·268 |
| | (1·536) | (2·545) | (1·143) | (15·6) | (21·2) | (5·3) | (0·105) |
| $n$-Butane (c1) | 1·296 | 2·342 | 1·261 | 23·3 | 24·0 | 8·7 | 0·253 |
| | (1·422) | (2·412) | (1·170) | (19·4) | (23·8) | (3·9) | (0·154) |
| $n$-Butane (c2) | 1·290 | 2·391 | 1·271 | 20·8 | 21·1 | 38·7 | 0·271 |
| | (1·491) | (2·521) | (1·154) | (15·5) | (20·2) | (31·9) | (0·124) |

$q_{ct}$, quantum of charge transfer from alkane to carbene at the TSs

**Table 4.** Selected geometrical parameters (distances in Å, angles in degrees, and barriers in kcal/mol) at the TSs of $^1$CCl$_2$ with alkanes at B3LYP (MP2)/6-31g ($d$, $p$).

| Alkane | $\tau_{C1H1}$ | $r_{C1C2}$ | $r_{C2H1}$ | $\theta_{H1C1C2}$ | $\theta_{H1C2C1}$ | $\phi_{C1H1C2H2}$ | $q_{ct}$ |
|---|---|---|---|---|---|---|---|
| Methane | 1·176 | 2·255 | 1·430 | 33·5 | 27·0 | 0·02 | 0·297 |
| | (1·203) | (2·250) | (1·345) | (29·7) | (26·3) | (0·0) | (0·316) |
| Ethane | 1·164 | 2·293 | 1·461 | 33·0 | 25·7 | -3·5 | 0·337 |
| | (1·199) | (2·276) | (1·349) | (28·5) | (25·1) | (2·2) | (0·353) |
| $n$-Propane(c1) | 1·164 | 2·291 | 1·461 | 33·1 | 25·8 | 0·7 | 0·336 |
| | (1·201) | (2·278) | (1·348) | (28·4) | (25·1) | (0·1) | (0·352) |
| $n$-Propane(c2) | 1·143 | 2·413 | 1·532 | 29·9 | 21·8 | 1·1 | 0·354 |
| | (1·187) | (2·379) | (1·380) | (23·9) | (20·4) | (3·3) | (0·375) |
| $n$-Butane (c1) | 1·163 | 2·295 | 1·470 | 33·3 | 25·8 | 4·0 | 0·342 |
| | (1·199) | (2·277) | (1·350) | (28·5) | (25·1) | (2·9) | (0·361) |
| $n$-Butane (c2) | 1·141 | 2·415 | 1·546 | 30·6 | 22·1 | 2·5 | 0·358 |
| | (1·184) | (2·375) | (1·389) | (24·6) | (20·8) | (3·9) | (0·385) |

$q_{ct}$, quantum of charge transfer from alkane to carbene at the TSs

sition states analyzed resemble the reactants rather than the products.[29] The proximity of the transition states to the reactants deviates with the degree of chlorination of carbene. Irrespective of the level of theory (B3LYP or MP2) followed, the insertions of $^1$CHCl form the transition states are 'earlier' than those of $^1$CCl$_2$ insertions as revealed by exothermicity values (table 2).

### 3.4 Transition state geometries

The relevant computed data for all the transition states have been presented in tables 3 and 4. A scrutiny of the bond breaking and bond formation steps corresponding to C2–H1 and C1–H1 respectively during the insertion process reveals that it is a con-

certed reaction. It is observed that the maturity of C1–H1 bond takes place earlier than the C1–C2 bond in the TSs (tables 3 and 4). The C1–H1 distances are inversely related to the barrier heights as expected. A similar relationship is also obvious in the C1–C2 distances (tables 3 and 4). The C2–H1 distances in the bond breaking process in all the transition states for $^1$CHCl insertions at B3LYP (MP2)/6-31g ($d$, $p$) have been found to be ~ 1·264 (1·197) Å and 1·272 (1·149) Å, respectively for primary and secondary C–H of higher alkanes. This shows again the belated transition states compared to that of $^1$CH$_2$ insertions.[11] The mean glide angle ($\theta_{H1C2C1}$) decreases from primary to secondary C–H of the alkane (table 3) and it gets reflected in the corresponding activation barriers (table 1). Further correlation is also no-

ticed when the torsion angles $\phi_{C1H1C2H2}$ have been analysed (table 3). The quantum of charge transfer from alkane to carbene in TSs increases with the increase in the number of alkyl substituents on the C2 carbon (table 3). It shows the inverse relationship between the barrier height and quantum of charge transfer. The same trend is observed in the case of $^1CCl_2$.

### 3.5 *NBO analysis*

NBO analysis of charge distribution in the transition states provides useful insights on the insertion reactivity. For all the transition states the second-order perturbative analyses were carried out for all possible interactions between filled Lewis-type NBOs and empty non-Lewis NBOs. These analyses show that the interaction between the $\sigma_{C2–H1}$ bond of alkane and the empty $p_\pi$ orbital of the carbenic–carbon ($\sigma_{CH} \rightarrow P_C$) and the charge transfer from the pair of electrons of the carbenic–carbon to the anti-bonding orbital of C2–H1 ($n_C \rightarrow \sigma^*_{CH}$) seems to give the strongest stabilization. Finally, we observed that there was a net charge flow from the alkane unit to the inserting chlorocarbene moiety. The quantum of charge transfer from alkane to carbene supporting the donor–acceptor interaction in the transition states for all the insertion reactions have been collected in tables 3 and 4. The inverse relationship between the quantum of charge transfer and the activation barriers reveals the fact that for the favorable insertion, the nucleophilicity of the alkane should have been enhanced either sterically or electronically. This correlation holds good for all the reactions analysed in this investigation. For example, in the case of $^1CCl_2$ insertion into *n*-butane at MP2 level the barrier heights, 11·9 and 8·0 kcal/mol, for the primary and secondary C–H bonds correlate with the charge transfer of 0·361 and 0·385 a.u. respectively.
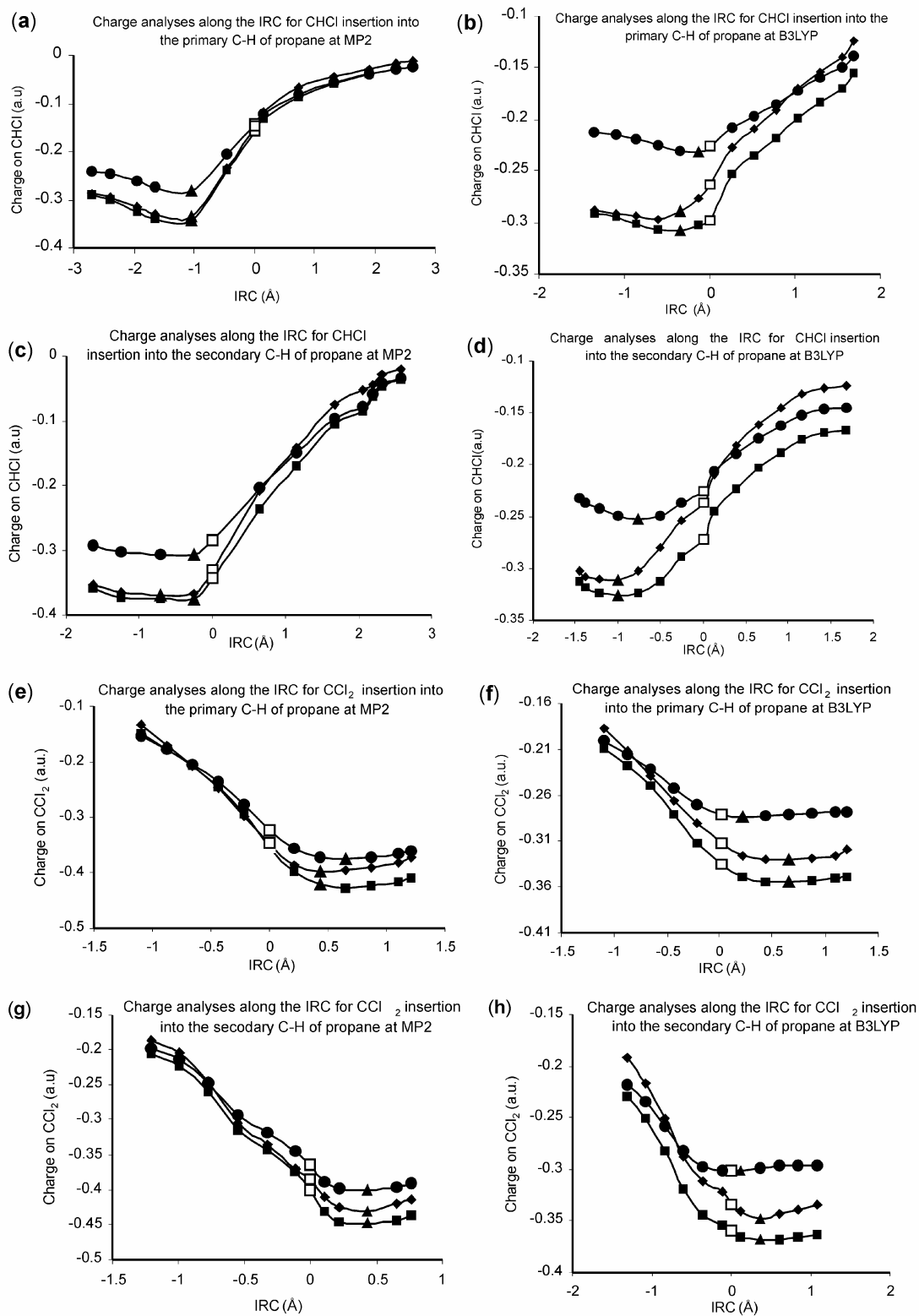
### 3.6 *IRC – charge analysis*

The total charge on the Chlorocarbene moiety along the IRC for the insertion reactions into the primary and secondary C–H bonds of propane, as calculated by Mulliken,[22] NPA[23] and CHelpG[24] methods using theoretical models has been shown in figure 2. Density functional (B3LYP) plots showing charge on the carbene moiety have been chosen in addition to the MP2 plots, which serve as our *ab initio* standard.

We discuss first the insertion reactions into the primary C–H bond of propane, $^1CClX$ (X = H, Cl) +

$CH_3–CH_2–CH_3$. The charge/IRC curves of these reactions are shown in figure 2. These reactions provide clear evidence for the two-phase (electrophilic/nucleophilic) mechanism in that there is a distinct turning point (charge minimum) in all the charge/IRC curves for the two Hamiltonians (MP2 and B3LYP) regardless of the model used to compute the atomic charges. For the $^1CHCl$ insertion (figures 2a and 2b), the turning point occurs after the transition state (TS), whereas with $^1CCl_2$ (figures 2e and 2f) the turning point occurs just before the TS. Thus for the $^1CHCl$ insertion, the TS occurs in the electrophilic phase whereas for $^1CCl_2$ the TS is reached near the starting point of the nucleophilic phase. This indicates that the TS for the insertion of $^1CHCl$ into the primary C–H bond of propane occurs much earlier along the reaction coordinate than does the TS for the corresponding $^1CCl_2$ insertion. This indication is fully supported both by the two TS geometries – for example, the C–H bond undergoing the insertion is much shorter in the $^1CHCl$ (1·172 Å) TS than in the TS for $^1CCl_2$ (1·348 Å) insertion (tables 3 and 4) and by the heat of reaction (table 2) and barrier height (table 1), which are more negative and much smaller, respectively for $^1CHCl$ (–97·66; 3·22 kcal/mol respectively) than for $^1CCl_2$ (–81·48; 12·60 kcal/mol respectively). This is in agreement with the Hammond postulate.[29] From the viewpoint of reactivity, it may be said that the vacant *p*-orbital on $^1CHCl$ is more available than that on $^1CCl_2$, thus facilitating the initial electrophilic phase of the reaction. In other words, reactivity increases in the order $^1CCl_2 < ^1CHCl$. There is an agreement in the overall shape and 'depth' of the curves themselves between the MP2 and B3LYP plots. However, the turning points in the B3LYP plots are less pronounced. The NPA and CHelpG curves are similar in shape at MP2 and B3LYP levels.

In the case of insertions of $^1CHCl$ into secondary C–H of propane, the position of the turning points and the charge/IRC curves (figures 2c and d) are very similar to that in the insertion into primary C–H of propane. The early TS for insertion into secondary C–H on comparison with that of primary C–H of propane is obvious from the TS bond distance of C–H undergoing insertion (table 3). But for $^1CCl_2$ insertion into secondary C–H of propane (figures 2g and 2h), the TS is observed near the starting point of the nucleophilic phase conforming the belated TS formation in comparison to the TS for insertion of $^1CHCl$ (figure 2c and 2d). The MP2 and B3LYP

**Figure 2.** (■) NPA; (●) Mulliken and (◆) CHelpG charge analysis respectively; (□) and (▲) correspond to the transition state and turning point respectively; Electrophilic phase- region right to the turning point; Nucleophilic phase-region left to the turning point.

curves for insertion into the primary and secondary C–H of propane are similar for all the three methods of computing the atomic charges. In general, the nucleophilic phase dominates for $^1CCl_2$ insertions, whereas the electrophilic phase dominates for $^1CHCl$ insertions.

## 4. Conclusions

The singlet chlorcarbenes insertions into the primary and secondary C–H bonds of alkanes have been analysed and the influence of chlorine substitution on carbenes on the transition states, energetics, geometrical parameters, etc. has been investigated both at B3LYP and MP2 levels. Both the theories predict that the activation barrier is a function of the degree of chlorination of carbene and the type of C–H into which insertion occurs. Among the two different types of carbene moiety approaches, i.e., $\sigma$ and $\pi$, the $\sigma$ approach is preferred over the $\pi$ approach at both levels of theory as the $\pi$ approach leads to the eclipsed conformation which is a second order saddle point. The NBO analyses have been done with a view to analysing the charge transfer processes during the insertion reactions. The charge/IRC plots provide clear evidences for the two-phase mechanism namely: an electrophilic phase and a nucleophilic phase for insertions of both $^1CHCl$ and $^1CCl_2$ into the primary and secondary C–H of propane respectively. Both B3LYP and MP2 methods give the similar picture of the investigated insertion reactions for geometries and heats of reaction.

## Acknowledgements

## References

1. Drake S A, Standard J M and Quandt R W 2002 *J. Phys. Chem.* **A106** 1357
2. Davies H M L, Hansen T and Churchill M.R 2000 *J. Am. Chem. Soc.* **122** 3063
3. Fischer E O and Maasbol A 1964 *Angew. Chem. Int. Ed. Engl.* **3** 580
4. Brahms D L S and Dailey W P 1996 *Chem. Rev.* **96** 1585
5. Storer J W and Houk K N 1993 *J. Am. Chem. Soc.* **115** 10426
6. Gleiter R and Hoffmann R 1968 *J. Am. Chem. Soc.* **90** 1475
7. Irikura K, Goddard III W A and Beauchamp J L 1992 *J. Am. Chem. Soc.* **114** 48
8. Russon N, Siclia E and Toscano M 1992 *J. Chem. Phys.* **97** 5031
9. Jorgensen W Land Salem L 1973 *The organic chemist's book of orbitals* (New York: Academic Press)
10. Von W, Doering E and Prinzbach H 1959 *Tetrahedron* **6** 24
11. Ramalingam M, Ramasami K, Venuvanalingam P and Sethuraman V 2005 *J. Mol. Struct.* (*Theochem.*) **755** 169
12. Fukui K 1970 *J. Phys. Chem.* **74** 4161
13. Frisch M J *et al* 2004 Gaussian 03 (Revision C.02) Gaussian Inc., Wallingford CT
14. Lee C, Yang W and Parr R.G 1988 *Physical Rev.* **B37** 785
15. Becke A D 1988 *Phys. Rev.* **A38** 3098
16. Miehlich B, Savin A, Stoll H and Preuss H 1989 *Chem. Phys. Lett.* **157** 200
17. Becke A D 1993 *J. Chem. Phys.* **98** 5648
18. Becke A D 1996 *J. Chem. Phys.* **104** 1040
19. Franel M M, Pietro W J, Hehre W J, Binkley J S, DeFrees D J, Pople J A and Gordon M S 1982 *J. Chem. Phys.* **77** 3654
20. Hariharan P C and Pople J A 1972 *Chem. Phys. Lett.* **66** 217
21. Gonzalez C and Schlegel H.B 1990 *J. Chem. Phys.* **94** 5523
22. Mulliken R .S 1955 *J. Chem. Phys.* **23** 1833
23. Reed A E, Weinhold F and Curtiss L A 1988 *Chem. Rev.* **88** 899
24. Breneman C M and Wiberg K B 1990 *J. Comput. Chem.* **11** 361
25. Bach R D, Su M D, Aldabbagh E, Andres J.L and Schlegel H B 1993 *J. Am. Chem. Soc.* **115** 10237
26. Bach R D, Andres J L, Su M D and McDouall J J W 1993 *J. Am, Chem. Soc.* **115** 5768
27. Gilles M K, Lineberger W C and Ervin K M 1993 *J. Am. Chem. Soc.* **115** 1031
28. Glendening E D, Reed A E, Carpenter J E, Weinhold F and Curtiss L .A 1988 *Chem. Rev.* **88** 899
29. Hammond G S 1955 *J. Am. Chem. Soc.* **77** 334